


Research Article

Implication of Radon Monitoring for Earthquake Surveillance Using Statistical Techniques: A Case Study of Wenchuan Earthquake

Aftab Alam,^{1,2} Nanping Wang ,^{1,2} Guofeng Zhao,³ and Adnan Barkat⁴

¹Key Laboratory of Geo-Detection, Ministry of Education, China University of Geosciences, Beijing, China

²School of Geophysics and Information Technology, China University of Geosciences, Beijing, China

³China Earthquake Network Centre, Beijing, China

⁴Centre for Earthquake Studies, National Centre for Physics, Islamabad, Pakistan

Correspondence should be addressed to Nanping Wang; 1996010992@cugb.edu.cn

Received 9 August 2019; Revised 30 December 2019; Accepted 4 February 2020; Published 9 March 2020

Academic Editor: Paolo Madonia

Copyright © 2020 Aftab Alam et al. This is an open access article distributed under the Creative Commons Attribution License, which permits unrestricted use, distribution, and reproduction in any medium, provided the original work is properly cited.

The seismotectonically induced changes in groundwater radon (Rn) are considered to be strong imputes for the surveillance of imminent major earthquakes. Groundwater facilitates the migration of soil gases as a result of tectonic stresses. In this regard, a radon time series is statistically analysed to identify the radon anomalies possibly induced by Wenchuan earthquake. The statistical analysis mainly involves the deterministic analysis of the Rn data and residual Rn analysis using a criterion ($\bar{x} \pm 2\sigma$) of anomaly selection having a confidence interval of 95%. The deterministic analysis reveals that the Rn time series follows a persistent trend ($0.5 \leq H \leq 1$) which confirms the absence of a chaotic regime. On the other hand, the residual Rn shows a notable upsurge straddling the time of the Wenchuan earthquake in the form of pre- and post earthquake changes at monitoring stations having $R_E/R_D \leq 0.3$. The residual Rn level passes the anomaly selection criterion ($\bar{x} \pm 2\sigma$) and is declared as a tectonically induced Rn anomaly. Contrary to this, the response of distant monitoring stations ($R_E/R_D > 0.3$) to this particular earthquake further validates the link between Rn and earthquake activity. In a nutshell, the present study highlights the potential implications of earthquake-induced radon anomalies for earthquake prediction research.

1. Introduction

Over the past few decades, earthquake prediction research attracts the attention of the scientific community due to the devastating nature of this phenomenon. However, there is no obvious success so far, due to the involvement of many variables [1–4]. Therefore, it is imperative to conduct research in this direction to mitigate the associated geohazards and minimize the loss of life and property. In this regard, numerous retrospective studies highlight the presence of atmospheric, ionospheric, and hydrogeochemical processes accompanied by earthquake activity [5–16]. These accompanying processes are considered as earthquake precursors and observed globally [11, 14, 17–23].

Among them, the hydrogeochemical response of earthquake activity has been extensively studied for the last few

decades [24]. The hydrogeochemical studies mainly include the monitoring in water level changes, Rn variability in either air, soil, or groundwater, an emanation of soil gases (CO_2 , CH_4 , and He), and other constituents such as Cl^- , SO_4^{2-} , and HCO_3^- are also used as a forerunner to access the earthquake-induced changes [7, 10, 11, 24–27]. However, the use of Rn is globally preferred in comparison with other precursors due to its relatively long half-life and ease of predictability [14].

In the past few years, numerous physical models were proposed to explain earthquake precursors [1–3, 20, 28, 29]. For example, Pulinets and Ouzounov [3] proposed a Lithospheric-Atmospheric-Ionospheric-Coupling (LAIC) model that explains the synergy between earthquake activity and its precursors. According to the LAIC model, the relative movement of tectonic blocks leads to the generation of

tectonic stresses. Furthermore, Koike et al. [30] performed a laboratory experiment to verify the growth of Rn emissions as a result of compressional stresses. These tectonic stresses are responsible for opening and closing of microfractures/cracks that facilitate the migration of Rn from the crust to the upper surface by means of carrier fluids such as groundwater or other soil gases like CO_2 , CH_4 , or N_2 in a wide range of geological settings [20]. In particular, Cicerone et al. [2] reported a correlation between the concentration of Rn and the regional variation of stress/strain. In addition, numerous studies highlight the presence of notable Rn anomalies in groundwater around the time of earthquake activity [19, 31–33].

In connection to the above, the Tashkent earthquake (M 5.3; 1966) provided the first evidence of earthquake-induced Rn anomalies in groundwater and gave hope to research on earthquake precursors [34]. Several years' analysis of the Rn data shows a multifold increase in the Rn levels around the time of this particular earthquake, and the same patterns also repeated for its aftershocks over a short time scale [35]. Such an analogous behaviour of Rn, earthquake, and its aftershocks gives evidence of earthquake-induced Rn anomalies. Later, a successful prediction was made for the Haicheng earthquake (M 7.3; 1975) based on multiple datasets along with Rn as discussed by [36]. Similarly, Hirota et al. [37] observed a gradual increase in the Rn count two weeks prior to the Nagano Prefecture earthquake (M 6.8; 1984) 65 km away from its epicentre. Afterwards, Igarashi and Wakita [5] analysed the Rn anomalies associated with earthquake events occurring from January 1984 to December 1988 in Japan and its surrounding areas. Prior to correlating Rn with earthquakes, the Bayesian statistic was successfully applied to remove background variations along with a criterion for anomaly selection (2σ), event magnitude ($M \geq 6$), and epicentral distance ($D \leq 100$) from the monitoring site. Twenty Rn anomalies satisfied the anomaly selection criteria and exhibited notable pre- and post earthquake changes, respectively. The Kobe earthquake (M 7.2; 1995) was also preceded by a marked groundwater Rn anomaly at a 17 m deep observation well 30 km away from the epicentre [38]. Presently, numerous studies have reported the groundwater Rn anomalies and suggest a more detailed analysis of the Rn anomalies for a more reliable prediction of major devastating earthquakes [11, 17, 20, 27, 33, 35].

In this regard, the present study provides a detailed temporal analysis of the Rn fluctuations in groundwater straddling the time of the major (M_w 7.9) and shallow (depth ≈ 19 km) Wenchuan earthquake. The Wenchuan earthquake occurred on May 12, 2008, along the Longmenshan fault (31.0°N, 103.4°E) in Sichuan Province, China [39, 40]. It is the most destructive earthquake in China since the 1976 Tangshan earthquake [41]. This devastating event was responsible for thousands of casualties and massive destruction on a regional scale. The Wenchuan earthquake also triggered a large number of geohazards such as landslides, slope collapses, and debris flow that seriously damaged counties in Sichuan Province, China [42, 43]. Given the devastation caused by this event, it is imperative to increase knowledge on earthquake precursors in this region. Therefore, we have

analysed the groundwater Rn variations at near and distant locations. It is important to mention that numerous researches also analysed the fluctuations of different ground and space-based parameters; however, the systematic analysis of radon is absent. Therefore, the present study will help to establish a synergy between numerous parameters in the context of earthquake forecasting.

2. Seismotectonic Settings of the Investigated Region

Seismically, China is ranked among highly active regions of the world with extreme interplate seismicity. The famous plate tectonic theory is unable to explain this intraplate seismicity of China, which state the occurrence of earthquakes within a narrow plate boundary zone [44]. The historical catalogue of China reveals the occurrence of more than 1000 ($M > 6$) earthquakes since 23 A.D., with thirteen being classified as a major catastrophic ($M > 8$) event. A classic example of a devastating historical earthquake in China is the Huaxian earthquake (1556) which killed approximately 830,000 people and is considered the deadliest earthquake in human history [45]. The Tangshan earthquake (M 7.8; 1976) is the best-known example of a modern age event in China in terms of loss of life (killed $\sim 250,000$ people and injured millions) and property [46]. In particular, the seismicity of western China is mainly influenced by the Indo-Eurasian collision which is responsible for the generation of the E-W trending fault system [47, 48].

The key tectonic feature in this region is the Longmenshan fault (LMSF) that runs parallel (around 500 km long and 40–50 km wide) to eastern Tibet and Sichuan basin in the northeast and southwest directions [12]. The LMSF zone is mainly dominated by the Wenchuan-Maowen fault, the Yingxiu-Beichuan fault, and the Guanxian-Jiangyou fault (Figure 1) with several thrust faults resulting from the compression between the Yangtze craton and the eastern Tibetan Plateau [40]. Historically, only two notable earthquakes of moderate magnitude (M 6.5, 6.2) were recorded in 1657 and 1956 along the LMSF zone, and considered as seismically inactive, until 2008 [40, 46], while Shi et al. [12] reported only one earthquake (M_w 6.1; 1989) on this fault. In 2008, the LMSF triggered a major (M_w 7.9) and shallow-focus (depth ≈ 19 km) Wenchuan earthquake (May 12, 2008) which gained the attention of the community in the capacity of reactivating the LMSF zone. The Wenchuan earthquake ruptured a 290 km long segment of the LMSF in total. This rupture is propagated 270 km unilaterally in the NE direction and 20 km in the SW direction with 80 km coseismic surface rupture. The Wenchuan earthquake resulted from the change of the LMSF dip angle (30° – 50° SW to 60° – 70° NE) and fault motion (SW thrusting motion to NE strike-slip motion) as provided commonly in various proposed slip models and summarized by [40].

The Wenchuan earthquake led to an estimated 69,225 casualties, 374,640 injuries, 17,939 missing, and approximately 5 million people left homeless. It is considered the second most destructive earthquake of this century after the great Sumatra earthquake in 2004 [41]. The Wenchuan

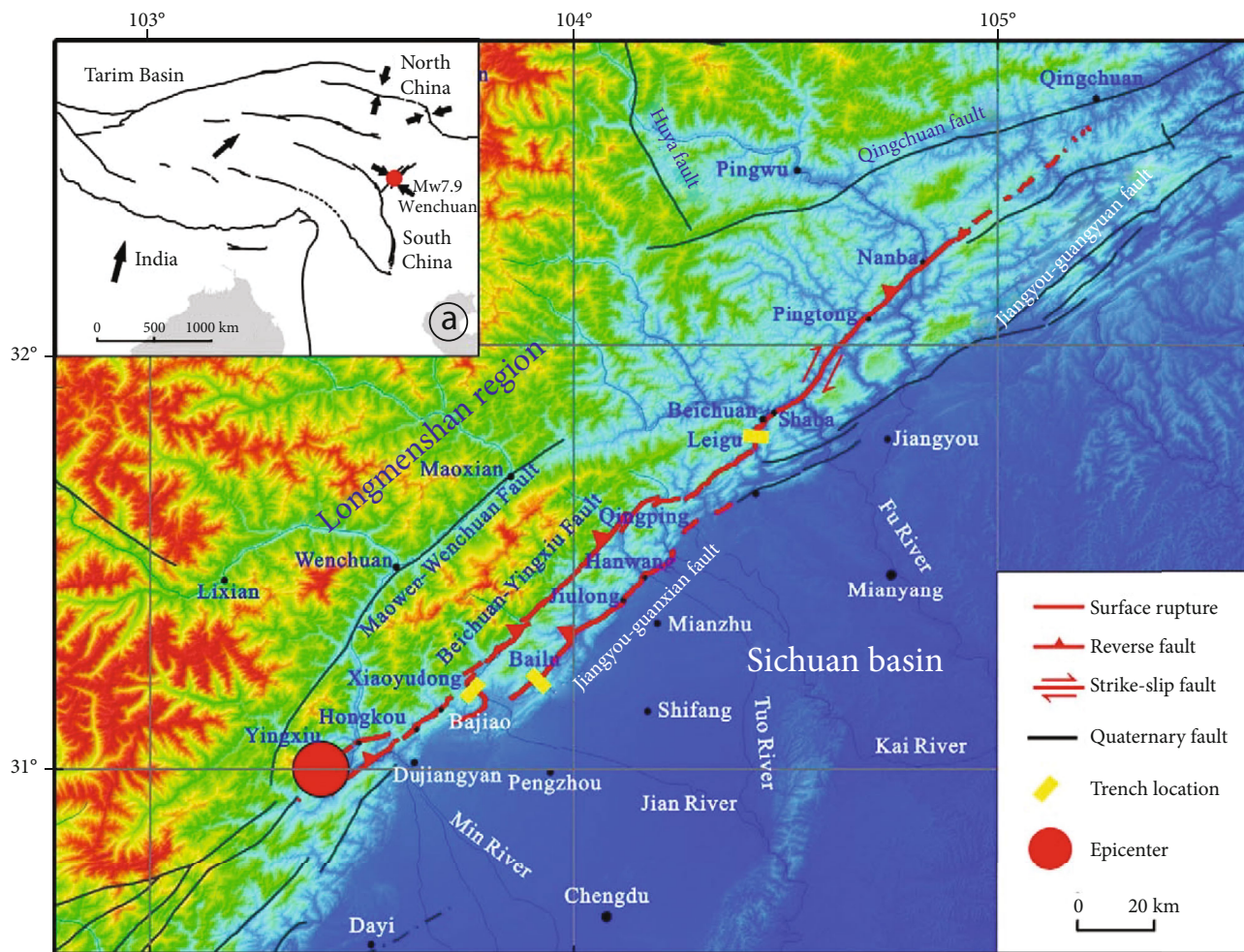


FIGURE 1: Epicentre location of Wenchuan earthquake Mw 7.9 along with surface rupture and important geological faults; the big red circle represents the epicentre, and trenching locations are represented by yellow rectangles. (a) represents the regional tectonic map, black arrows showing the direction of plate movement [49].

earthquake was followed by more than 10,000 aftershocks of $M \geq 2.0$ that lasted until Dec 31, 2008 [50]. This devastating earthquake was also responsible for the triggering of more than 15,000 geohazards (landslides, rockfall, and debris flow) which resulted in about 20,000 casualties [39]. The destruction caused by the event highlights the importance of earthquake precursory studies in seismically active regions to minimize the loss of life and property.

3. Methodology

The methodology adopted in the current study is divided mainly into two stages: (a) instrumental setup and (b) theoretical setup. The instrumental setup explains the strategy adopted for the data collection and a brief description of the instrument used for radon monitoring, while the theoretical setup explains about the statistical analysis of radon data for identification of radon anomalies possibly induced by earthquake activity.

3.1. Instrumental Setup. Since 1966, immediately following the Xingtai earthquake sequence (March 22, 1966), China

has started an organized, persistent, and systematic effort to testify the postulate of preearthquake anomalies in the context of earthquake forecasting by the China Earthquake Administration (CEA). This research programme was primarily focused on earthquake prediction and its implications to minimize the irrevocable destruction posed by major earthquakes. The CEA has mainly classified this research programme into the following classifications: imminent (weeks to days, even hours), short (months to weeks), medium (years), and long-term (decades) earthquake forecasting. In this regard, the CEA has installed seismological, geodetic/geoelectric/geomagnetic, ground fluid, and hydro-seismological networks for monitoring potential earthquake precursors [42].

In particular, the CEA is operating a very dense radon monitoring network for the surveillance of earthquake activity. For earthquake forecasting research, Rn is more preferred due to its comparatively longer half-life and easy detectability [14]. In the current study, we have analysed the variations of continuous groundwater Rn concentration associated with the devastating Wenchuan earthquake (May 12, 2008; Mw 7.9) at 9 stations over the whole year (2008) in the proximity

of the event epicentre. The details of the Rn monitoring stations regarding its location and distance from the event epicentre are presented in Table 1.

The Rn data used in the current research was acquired by means of two instruments. For automatic continuous sampling, the mixture of escaped gas and water coming from well was passed through a degasser and gas-collecting device and then collected into a ZnS (Ag) detector system for Rn concentration measurement. This is a digitized method of measurement, and the observation equipment is mainly SD-3A with sampling interval of one hour and a measurement precision of 0.1 Bq/L. For the acquisition of the daily variation in Rn concentration, water from the well was sampled and degassed by bubbling degassing and then transported into an ion chamber or ZnS (Ag) detector, where the Rn concentration was measured by an ionization or scintillation method using FD-125 instrument. The measurement precision is also 0.1 Bq/L with a sampling interval of one reading per day. The further detail of instrumental setups used for Rn monitoring is provided by [51]. Precipitation is not monitored by the CEA for all the stations used in the current research, and therefore, such data is not available. To overcome this issue, the precipitation dataset of the Tropical Rainfall Measuring Mission (TRMM) satellite for the year 2008 was utilized in this paper. The TRMM dataset was considered as the best solution among the available sources of precipitation data for China. The negative correlation observed between groundwater Rn anomalies and rainfall for the whole year and the selected time frame is presented in Table 2.

3.2. Theoretical Setup

3.2.1. Fractal Analysis of Radon Data. The dynamics of the Rn time series show a very complex nonlinear temporal pattern normally characterized by nonstationary and multiscale features [52]. This chaotic regime of the time series is realized through diurnal, seasonal, multiyear, and decadal Rn cycles along with key influencing parameters [14, 53, 54]. Therefore, the Rn time series is subjected to fractal estimates to determine the degree of chaotic behaviour of Rn and intrinsic long-memory correlations, if any [55]. Besides this, the estimation of fractal elements for the Rn time series leads to further exploration of the underlying dynamics of physical systems such as seismic activity [56]. In this regard, the fractal quantity known as the Hurst exponent (H) is calculated for the Rn time series using the rescale-range (R/S) analysis. The estimation of H is based on the following relationships:

$$\log \left(\frac{R}{S} \right)_s = \text{constant} + H \log s, \quad (1)$$

where R is the range, S is the standard deviation, H is the Hurst exponent, and s is the number of entries in a group.

$$\left(\frac{R}{S} \right)_s = \frac{1}{d} \sum_{k=1}^d \left(\frac{R_{k,s}}{S_{k,s}} \right), \quad (2)$$

where

$$S_{k,s} = \sqrt{\frac{\sum_{i=1}^s \left(X_{(k-1)s+i} - \bar{X}_{k,s} \right)^2}{s}}, \quad (3)$$

$$R_{k,s} = \max_{1 \leq i \leq s} \{ (Y_{k,s})_i \} - \min_{1 \leq i \leq s} \{ (Y_{k,s})_i \}. \quad (4)$$

Here, the set of observations ($N \in \{N_1, N_2, N_3, \dots, N_n\}$) is divided into d nonoverlapping intervals of X , ($X_{(k-1)s+1}, X_{(k-2)s+2}, \dots, X_{k,s}$), whereas $k = 1, 2, 3, \dots$,

d with individual length = n/d . Afterwards, the Rn time series is categorized as antipersistent ($0 \leq H \leq 0.5$), random ($H \approx 0.5$), and persistent ($0.5 \leq H \leq 1$) based on the obtained value of H . In particular, the antipersistency means that low present values will probably be followed by high figure values and vice versa. Persistency exhibits that a long-lasting autocorrelation exists within the time series, which implies that high present values will probably be followed by high future values and vice versa. And random walk means that they are uncorrelated or do not possess long memory trend [14, 56].

3.3. Identification of Radon Anomalies. The inspection of fractal dynamics of Rn time series allows for the identification of anomalous Rn variations if they exist. For reliable identification of an earthquake anomaly, the monitoring station must lie within the Earthquake Preparation Zone (EPZ). The EPZ is defined as an area within which the premonitoring fluctuations associated with the tectonically induced impending earthquake can be observed. In [57], an empirical relationship is proposed for EPZ (R_D ; km) based on the magnitude (M) of the earthquake event, given as

$$R_D = 10^{0.43M}, \quad (5)$$

where the epicentral distance (R_E ; km) between the monitoring site and the event epicentre is calculated as

$$R_E = D \times R, \quad (6)$$

where

$$D = \cos^{-1} \left(\cos \alpha_i \cos \alpha_j + \sin \alpha_i \sin \alpha_j \cos (\beta_i - \beta_j) \right). \quad (7)$$

Here, α_i, β_i are the coordinates of the earthquake event, α_j, β_j are the coordinates of the Rn monitoring station, and $R \approx 6370$ km is the earth's radius [58]. In an ideal scenario, only those events having $R_E/R_D \leq 1$ are considered for earthquake forecasting studies. In our case, all the stations are lying within (R_D) as proposed by [57] and adopted in numerous studies [14, 18, 22].

In addition to all the above, the acquired groundwater Rn data is investigated for identification of anomalous periods possibly linked with this particular event. The recognized anomalous periods mainly lie around the time of the earthquake within a time window of ± 3 months (Mar to Jul

TABLE 1: List of Rn monitoring stations used in the current study along with their location and distance from the event epicentre.

Sr. No.	Station code	Station name	Latitude (°N)	Longitude (°E)	Epicentral distance (R_E ; km)	$\frac{R_E}{R_D}$
01	MSS	Mingshan	30.10	103.10	105.6	0.0423
02	MXS	Maoxian	32.05	103.55	115.7	0.0463
03	KDS	Kangding	30.12	102.17	152.2	0.0610
04	SPS	Songpan	32.65	103.60	182.5	0.0731
05	GS	Ganzi	31.61	100.01	325.5	0.1305
06	ZJS	Zhaojue	28.00	102.82	340.1	0.1363
07	PZHS	Panzhihua	26.51	101.74	526.0	0.2109
08	YQS	Yanqing	40.50	115.90	1542.9	0.6184
09	SYS	Shunyi	40.21	116.50	1563.2	0.6267

TABLE 2: Pearson's correlation coefficient (r^2) for the relation of rainfall and the groundwater Rn for stations used in the current research showing a negative correlation.

Sr. No.	Station code	Whole year correlation	Selected time window correlation
1	MSS	0.210	0.197
2	MXS	0.195	0.141
3	KDS	0.286	0.292
4	SPS	0.014	0.033
5	GS	0.182	0.208
6	ZJS	-0.013	-0.085
7	PZHS	-0.036	0.044
8	YQS	0.059	0.119
9	SYS	0.048	-0.038

2008). The rationale behind the selection of this flexible time window is to analyse the effect of whole aftershock sequence of the Wenchuan earthquake. The identified anomalous periods were further analysed using residual signal processing techniques to eliminate the regular filtering effect as indicated in numerous studies [14, 22, 59]. The residual Rn ($dA(t)$) is calculated via a relationship given as

$$dA(t) = A(t) - RA(t), \quad (8)$$

where $A(t)$ is the daily average Rn concentration and $RA(t)$ is the 7-day rolling average Rn concentration. Furthermore, we have also applied a statistical criterion ($\bar{x} \pm 2\sigma$) of the anomaly selection on residual Rn having a confidence interval of 95% and is consistent with other studies [14, 18, 23, 60, 61].

4. Result and Discussion

The temporal variability of groundwater Rn was recorded from January to December 2008 near the LMSF zone at nine different locations in China. The data analysis reveals anomalous fluctuations of Rn at a few stations under normal meteorological conditions, which highlights the aspect of a tectonically induced Rn anomaly, while the inspection of the earthquake catalogue of this selected period owns the aspect of tectonically induced radon anomaly due to the

Wenchuan earthquake that occurred on May 12, 2008, in Sichuan, China. Details of the earthquake are presented in Table 3.

In this regard, we performed a detailed statistical analysis of Rn concentrations, in order to verify the possible correlation of the Rn anomalies with this particular event. The Rn monitoring stations included in the current study are presented in Figure 2.

It includes 9 stations lying within the EPZ of the Wenchuan earthquake installed by the CEA within the proximity of the LMSF zone (Table 1). The annual variation of Rn recorded at selected monitoring stations is presented in Figure 3.

Figure 3 indicates a few periods (April-June 2008) of abnormal rise and fall of Rn around the time of the Wenchuan earthquake. For example, the MSS station shows a sudden rise of the Rn level from 14.6 Bq/L to 19.4 Bq/L in the second week of May 2008 (Figure 3(a)). This rise in the Rn level continues onward throughout the whole year. Likewise, other monitoring stations such as MXS, KDS, GS, and SPS also reveal an anomalous change in real Rn requiring a detailed study (Figures 3(b)–3(e)). An analogous change of the Rn level was also observed at the relatively distant monitoring stations with $R_E/R_D > 0.5$ (Table 1; Figures 3(h) and 3(i)). Based on the results of the preliminary investigation, the anomalous periods of the Rn concentration are subjected to a detailed analysis. This detailed analysis includes the advanced residual signal processing techniques which remove the regular filtering effects from data if any. Besides this, a statistical criterion of $\bar{x} \pm 2\sigma$ is also applied to the residual Rn to further authenticate our results. The result of this detailed analysis is presented in two stages: (a) station is located very near to the event epicentre ($R_E/R_D \leq 0.3$) and (b) station is located far away from the event epicentre ($R_E/R_D > 0.3$) for comparison purposes.

Prior to analysing the Rn data for earthquake forecasting research, we have determined the dynamics of the Rn time series using fractal dimensions such a Hurst exponent. The Hurst exponent reveals that the time series follows a persistent trend ($0.5 \leq H \leq 1$) for all the Rn monitoring stations with insignificant fluctuations as presented in Figure 4. A positive autocorrelation is found to exist in the recorded Rn data. This suggests that the past trend of data is continued in the future and there is no existence of an irregular trend.

TABLE 3: Epicentral parameters of the Wenchuan earthquake, China.

Earthquake (case study)	Date (MM:DD:YYYY)	Magnitude (M_w)	Latitude ($^{\circ}$ N)	Longitude ($^{\circ}$ E)	Depth (km)	Preparation zone (R_D ; km)
Wenchuan, China	05:12:2008	7.9	31.021	103.376	19	2494

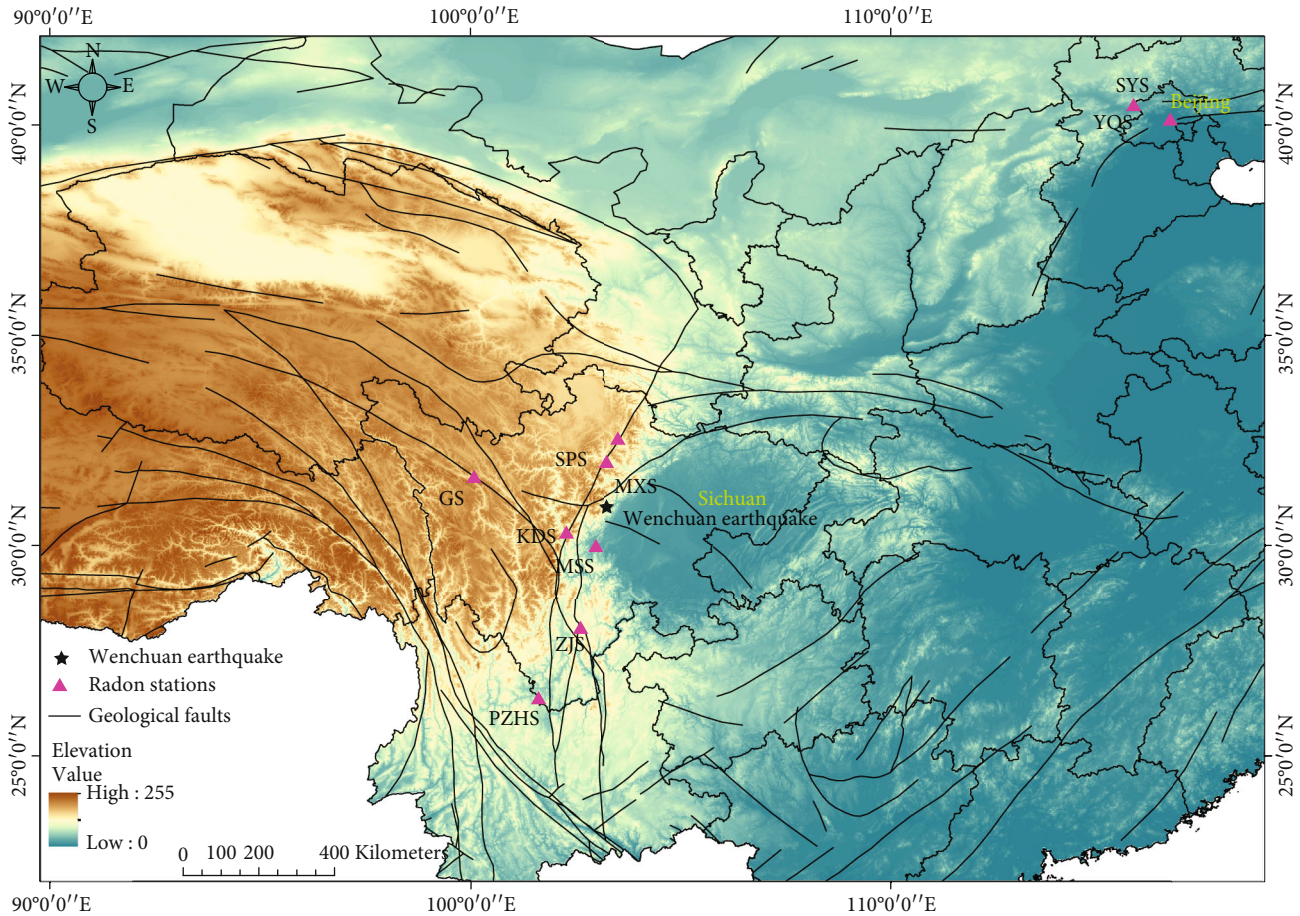


FIGURE 2: Regional tectonic map of China along with the location of the Rn monitoring stations and major faults. The black star shows the location of the Wenchuan earthquake.

At the first stage, detail analysis of Rn is performed for the station located near the event epicentre as presented in Figures 5 and 6. It includes 7 monitoring stations located in the proximity of the LMSF zone having ($R_E/R_D \leq 0.3$). Figure 5 illustrates the change of the residual Rn levels along with daily precipitation for MSS, MXS, KDS, and SPS stations. The temporal variation of the residual Rn concentration was observed from Mar 1 to June 30, 2018, along with daily precipitation records. The Rn levels seem to be within normal limits ($\bar{x} \pm 2\sigma$) until the occurrence of the Wenchuan earthquake on May 12, 2008. On May 12, 2008, the Rn levels breach the threshold of anomaly selection ($\bar{x} \pm 2\sigma$) and show a sudden upsurge from 0 to 2.4 Bq/L of the residual Rn and 13-18 Bq/L of daily Rn level (Figures 3(a)–5(a)). This particular change in the Rn level followed by the Wenchuan earthquake highlights the aspect of the post earthquake Rn anomaly, while the daily Rn variations recorded at the MXS

stations show a gradual increase in Rn from April to June 2008 with insignificant precipitation (Figures 3(b)–5(b)).

A detailed inspection of Rn shows that the residual Rn level passed the anomaly selection criteria prior to the Wenchuan earthquake. This preearthquake Rn anomaly seems to be absent after event occurrence (Figure 5(b)).

The KDS monitoring station shows unambiguous changes in the residual Rn levels around the time of this particular event (Figure 5(c)). Initially, this anomalous trend is observed 5 days prior to the Wenchuan earthquake on May 07, 2008, and continued until July 2008 showing post earthquake anomalies. It is important to mention that these post earthquake changes were possibly associated with the aftershock sequence of the Wenchuan earthquake [50]. Similarly, the SPS monitoring station having $R_E/R_D \approx 0.073$ and $R_E \approx 182$ km shows a multifold increase in the daily Rn levels around the time of the Wenchuan earthquake (Figure 3(d)).

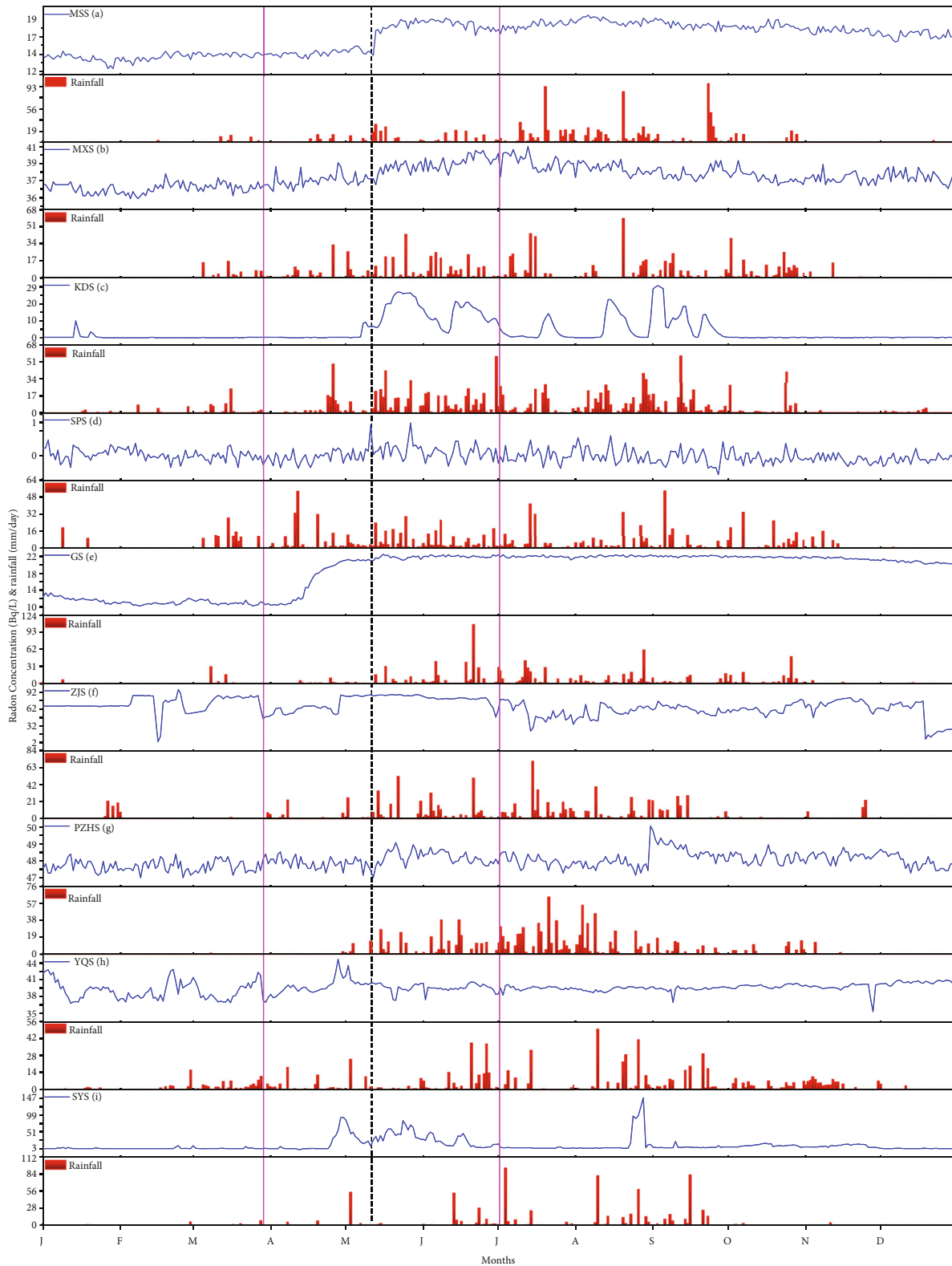


FIGURE 3: Temporal variation of groundwater Rn recorded at different stations in the proximity of the Wenchuan earthquake. A time window of 3 months (April-June 2008) is selected for detailed analysis of the Rn variability in connection with this particular earthquake (highlighted by a magenta colour dashed line column). It includes 9 stations in total with 7 stations located near the event epicentre and 2 stations located at distant locations (YQS and SYS stations in Table 1). The black dotted line is the time of the Wenchuan earthquake.

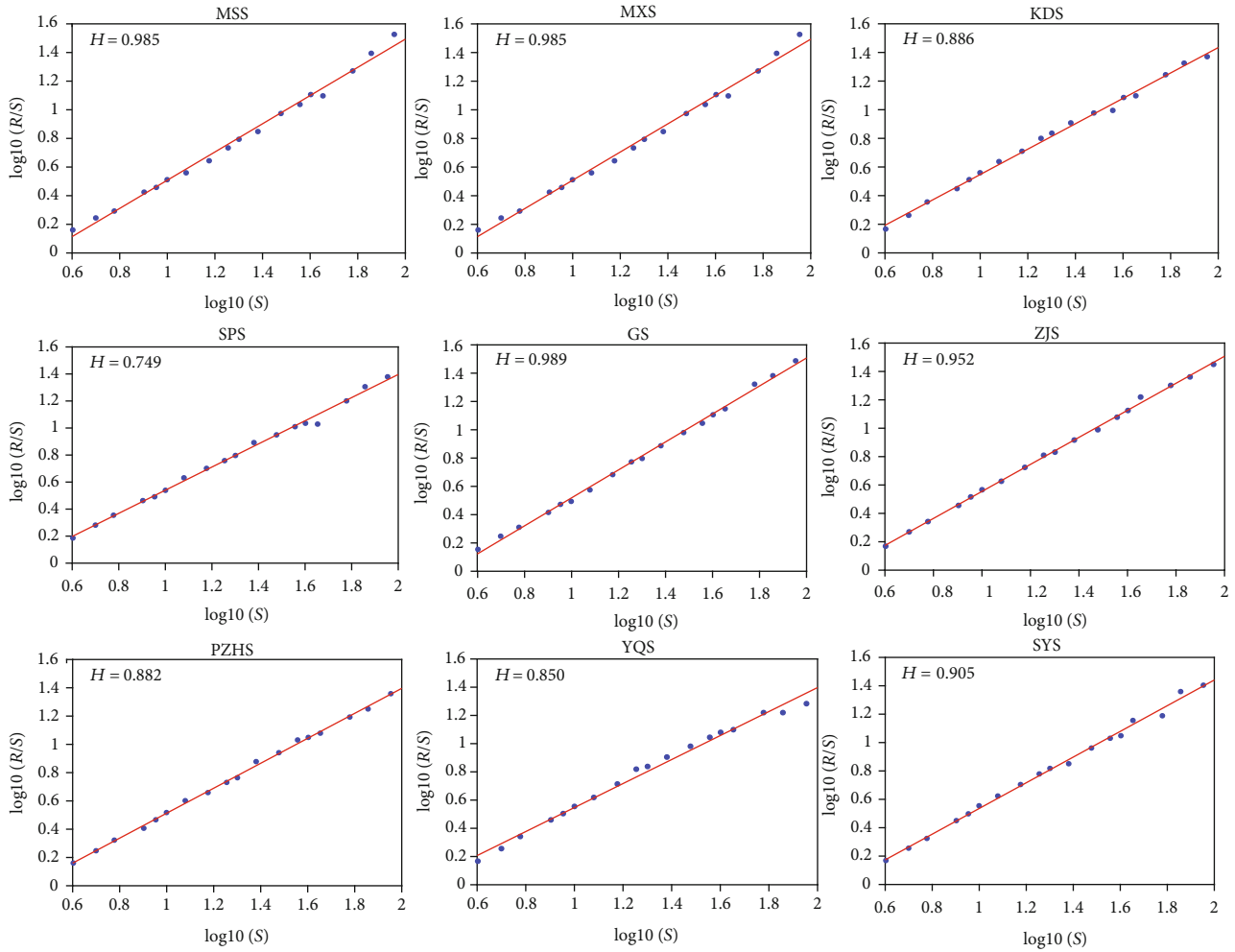


FIGURE 4: The H estimate of Rn time series recorded at different monitoring stations. The recorded Rn data inherent to the characteristics of long memory trend such as persistency ($0.5 \leq H \leq 1$). The H values lying within the range of 0.749 to 0.989 and show a trend continuation rather than trend reversion or white noise. In the case of white noise, the time series is no more favourable for retrospective analysis of earthquake forecasting.

The average Rn value recorded at the SPS monitoring station ranges between 0.2 and 0.3 Bq/L, while the peak value observed one day prior to the Wenchuan earthquake is nearly 0.52 Bq/L. Additionally, the residual Rn level of the SPS monitoring station overpasses the anomaly selection threshold which further authenticates its linkage with this particular event.

In continuation, the temporal variability of the residual Rn concentration for GS, ZJS, and PZHS monitoring stations is presented in Figure 6. The GS monitoring station reveals an unambiguous increase in the Rn levels prior to event occurrence within a very short interval of time (4-6 days). The Rn level range is within a limit of 11-13 Bq/L from Jan 2008 to the end of April 2008. Afterwards, a sharp increasing trend of Rn is observed from the beginning of May 2008 and continued onward (Figure 3(e)). This anomalous change is subject to detailed analysis via residual signal processing technique for reliable identification of tectonically induced Rn anomaly. The results of the residual Rn show development of an Rn anomaly overpassing the

anomaly selection threshold preceding the earthquake event (Figure 6(a)). Similarly, the other monitoring stations presented anomalous patterns of the daily and the residual Rn levels highlighting the aspect of tectonically induced Rn anomalies under favourable conditions (Figures 3(f), 3(g), 6(b), and 6(c)). Inclusively, all the monitoring stations lying around the proximity of the LMSF zone show Rn variations with varying amplitude in connection with this particular event.

At the second stage, the temporal variability of Rn is analysed for distant Rn monitoring station with $R_E/R_D > 0.3$ (Figures 3-6). It includes the YQS and SYS monitoring stations having R_E value 1542.9 km and 1563.2 km, respectively (Table 1). The temporal variability of raw Rn levels recorded at these monitoring stations shows an increasing trend around the time of the Wenchuan earthquake, despite its distant location (Figures 3(h) and 3(i)). The YQS monitoring station shows multiple peaks in Rn levels with varying amplitudes prior to the event's occurrence. The highest peak (44.2 Bq/L) of Rn levels is observed on May 1-2, 2008, around

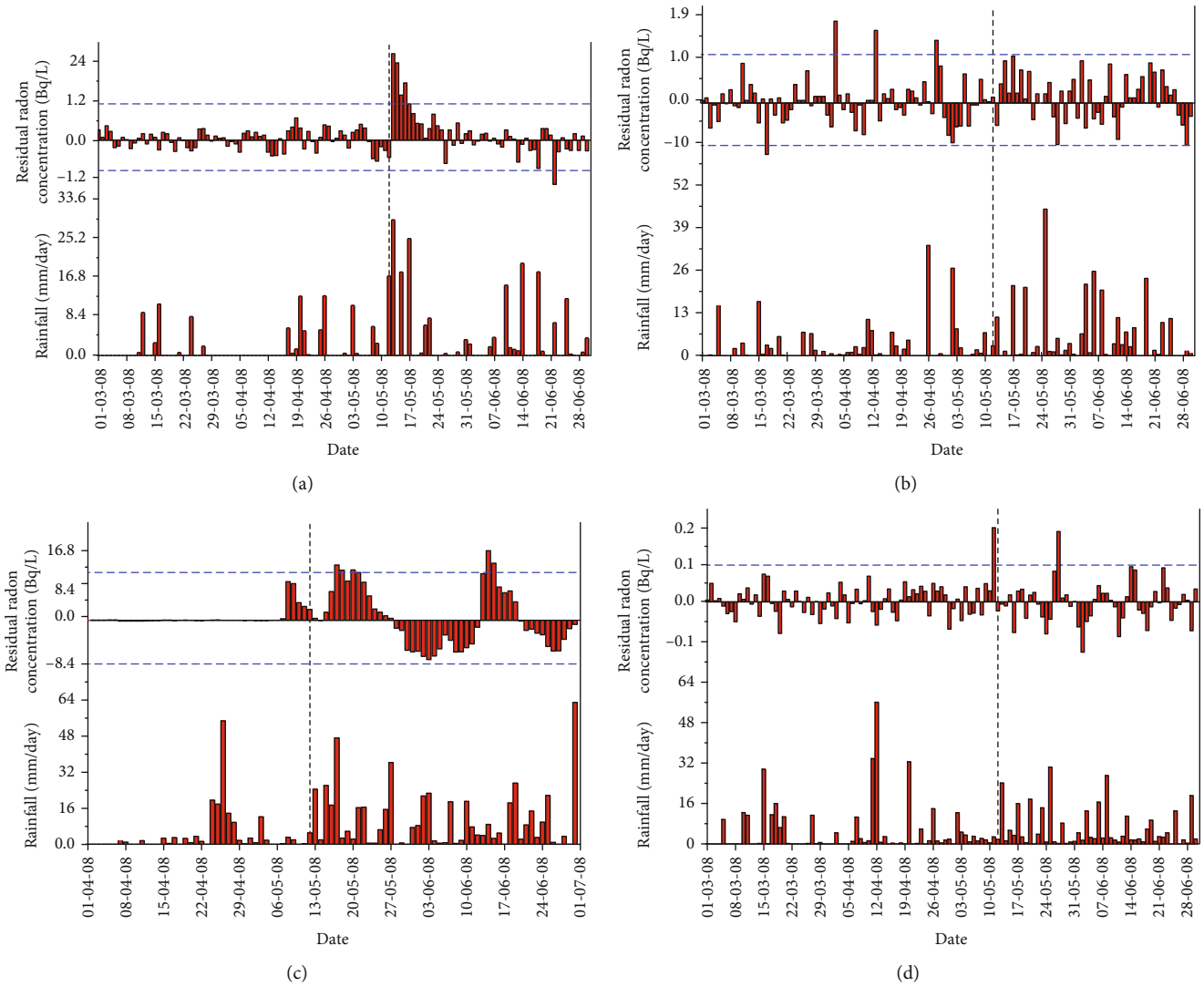


FIGURE 5: The results of the residual Rn time series for (a) MSS, (b) MXS, (c) KDS, and (d) SPS monitoring stations along with daily precipitation record. The MSS station shows a very notable change in the residual Rn overpassing the statistical criterion immediately following the Wenchuan earthquake (indicated by the dotted black colour vertical line) as co- and post earthquake Rn anomalies, while the rest of the stations exhibit both pre- and post earthquake signature with an insignificant level.

10-12 days prior to the Wenchuan earthquake, while the Rn levels remain within the normal limit (around mean value 39 Bq/L) for the rest of the period (Figure 3(h)). Likewise, the SYS station also shows an analogous change in the Rn levels around the time of this particular event (Figure 3(i)). These anomalous periods are further subjected to a detailed investigation as presented in Figures 6(a) and 6(b).

The residual Rn value of the YQS station shows a significant increase on April 30, 2008, and overpasses the statistical criterion of the anomaly selection. This anomalous change in residual Rn is followed by the Wenchuan earthquake that occurred 11 days later, while during the rest of the period Rn levels were found to be within normal limits (Figures 3(h) and 7(a)). On the contrary, the temporal analysis of the residual Rn at the SYS station also depicts a notable rise in Rn levels almost 12-15 days prior to this devastating earthquake (Figure 7(b)).

Moreover, the comparative analysis of rainfall for the whole year and selected days further confirms the connection of Rn abnormality with this particular event (Table 2).

It is important to mention here that the current results show an analogy with the earlier investigations of the preseismic process in connection with the Wenchuan earthquake [8, 12, 51, 62]. For example, Shi et al. [12] studied the hydrological response of the Wenchuan earthquake at near and distant monitoring stations. They reported significant evidence of hydrological changes such as water level in response to the Wenchuan earthquake. Similarly, Ren et al. [51] also analysed the postseismic changes in Rn levels at different geochemical observation points using step variation curves. Their findings confirm the change in aquifer parameters as a response of dynamic loading, which may help in designing an optimum strategy for earthquake forecasting. In addition to this, Ye et al. [62] monitored the Rn levels

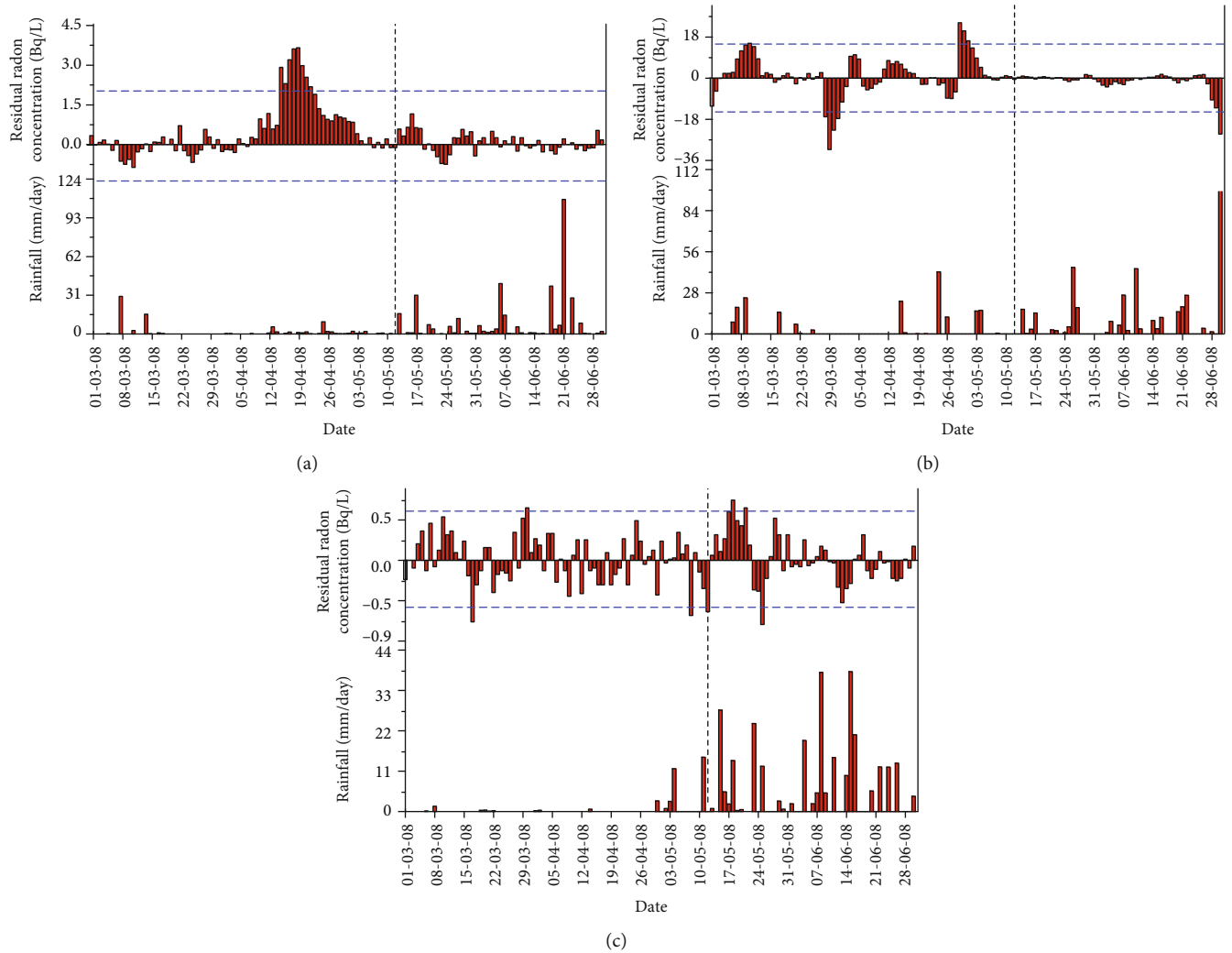


FIGURE 6: The results of the residual Rn time series for (a) GS, (b) ZJS, and (c) PZHS monitoring stations along with daily precipitation record. The GS monitoring station shows a very prominent possible preearthquake anomaly observed from April 12, 2008, to April 26, 2008. On the contrary, the ZJS and PZHS stations show multiple short-term Rn anomalies both preceding and succeeding this particular event. The black vertical dotted line indicates the time of earthquake occurrence.

in soil and water along with water level and temperature fluctuations along the Longmenshan fault zone. They observed that both the Rn concentration and water level show positive and negative relationships in response to the Wenchuan earthquake. Besides this, Liu et al. [8] analysed the seismoionospheric parameter (GPS total electron content (TEC)) in connection with the May 12, 2008, Wenchuan earthquake. It is observed that the GPS-TEC shows an anomalous decrease above the forthcoming epicentral region and gives a possible validation of the LAIC model. In general, the results of the present study are found to be in accordance with earlier investigations and reveal that Rn is a promising tool for earthquake forecasting research.

5. Conclusions

The present study encompasses the analysis of the groundwater Rn response associated with the devastating Wenchuan earthquake (Mw 7.9) that occurred on May 12, 2008, in

mainland China. On this subject, the daily variation of the Rn levels is recorded within the EPZ at multiple near and distant locations within the proximity of the LMSF zone that is responsible for the triggering of this particular event. Primarily, it is observed that the daily Rn levels show a notable change around the time of earthquake occurrence. The period of notable Rn variations is further subjected to the detailed analysis of Rn using statistical techniques for reliable identification of tectonically induced Rn anomalies. The key findings of the current investigation are summarized below:

- (a) The time series analysis of the groundwater Rn at different monitoring stations over the whole period (Jan-Dec 2008) reveals notable changes in Rn levels around the occurrence time of the Wenchuan earthquake. This notable response of groundwater Rn is observed at both near and distant monitoring stations having $R_E/R_D \leq 1$

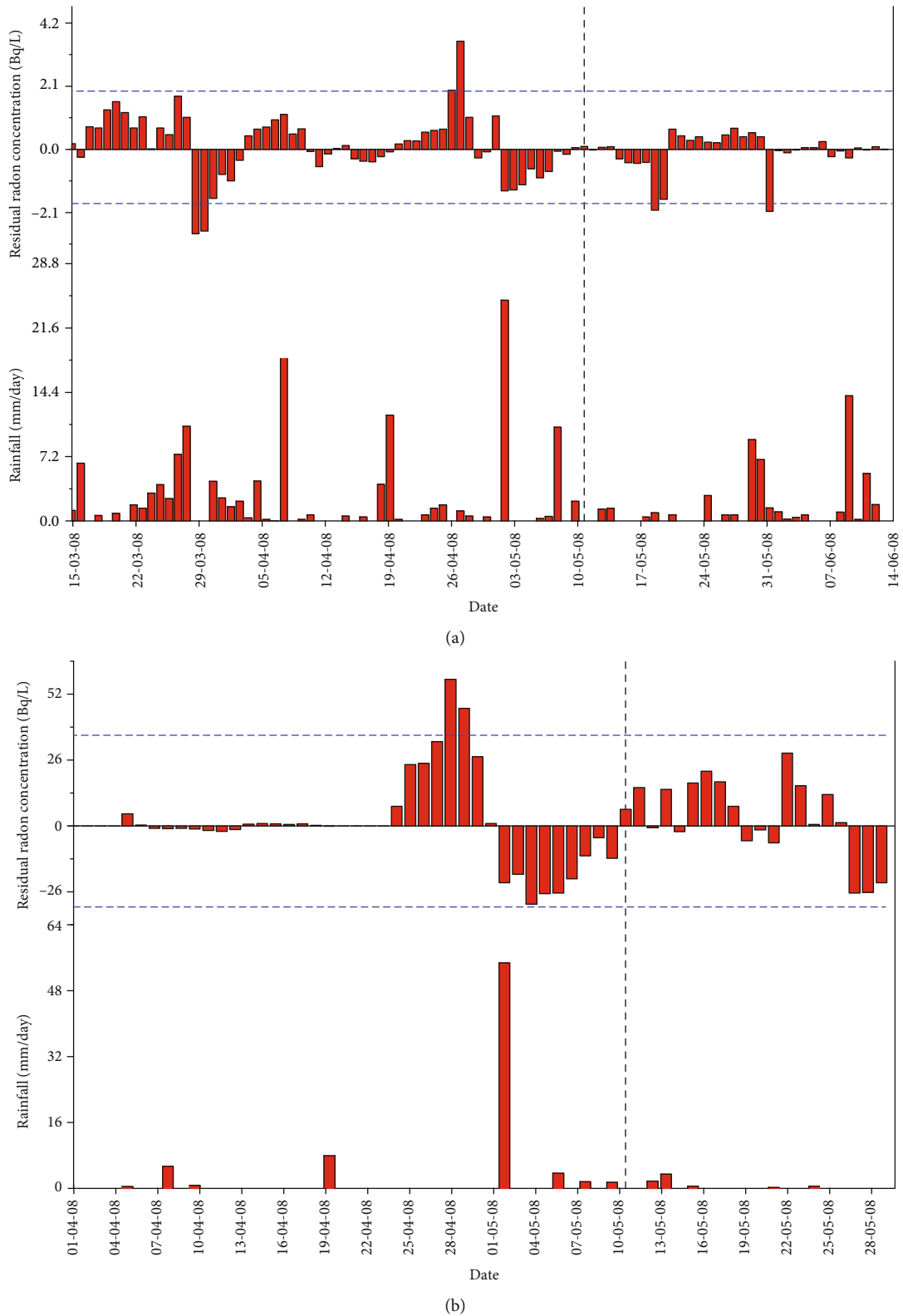


FIGURE 7: The fluctuation of residual Rn at two distant Rn monitoring stations: (a) YQS and (b) SYS having $R_E/R_D > 0.3$. The inspection of the residual Rn time series shows very notable changes in the Rn levels despite its comparatively longer distance from the event epicentre. The YQS station shows a short-term increasing and decreasing trend of Rn around the time of event occurrence, while the SYS station shows gradual increase and sudden decrease in residual Rn prior to the event occurrence. Such an abnormal change in level is found to be absent from the rest of the data as presented earlier. Such exceptional changes in the Rn levels are possibly induced due to tectonic stress associated with the major Wenchuan earthquake.

- (b) The deterministic analysis of the Rn time series suggests a positive autocorrelation with the absence of white noise in the dataset. The H exponent exhibits that the recorded data has a long memory correlation between past and future data points
- (c) The residual signal processing techniques were applied on observed periods of Rn enhancement for reliable identification of the Rn anomalies along with a statistical criterion of anomaly selection ($\bar{x} \pm 2\sigma$). The response of the residual Rn variations associated with this tectonic activity appears in the form of possible pre- and post earthquake Rn anomalies with variable amplitudes. The findings of the current study are consistent with earlier investigations

The analysis of the Rn time series shows a notable response possibly induced by tectonic origin that may effectively support the forecasting of impending catastrophic seismic events. Our results suggest that, on a global perspective, radon should be used as a potential seismic indicator for seismically active regions.

Data Availability

The data (groundwater radon) used to support the findings of this study belongs to China Earthquake Data Center and will be provided on demand from the relevant organization.

Conflicts of Interest

The authors declare no conflict of interest.

Acknowledgments

The authors would like to thank the China Earthquake Data Center (<http://data.earthquake.cn>) for providing the radon data. This study was supported by the National Natural Science Foundation of China (no. 41674111).

References

- [1] C. H. Scholz, L. R. Sykes, and Y. P. Aggarwal, "Earthquake prediction: a physical basis," *Science*, vol. 181, no. 4102, pp. 803–810, 1973.
- [2] R. D. Cicerone, J. E. Ebel, and J. Britton, "A systematic compilation of earthquake precursors," *Tectonophysics*, vol. 476, no. 3–4, pp. 371–396, 2009.
- [3] S. Pulinet and D. Ouzounov, "Lithosphere-Atmosphere-Ionosphere Coupling (LAIC) model - An unified concept for earthquake precursors validation," *Journal of Asian Earth Sciences*, vol. 41, no. 4–5, pp. 371–382, 2011.
- [4] G. Asencio-Cortés, F. Martínez-Álvarez, A. Morales-Esteban, J. Reyes, and A. Troncoso, "Improving earthquake prediction with principal component analysis: application to Chile," in *Lecture Notes in Computer Science*, vol. 9121, pp. 393–404, Springer, Cham, 2015.
- [5] G. Igarashi and H. Wakita, "Groundwater radon anomalies associated with earthquakes," *Tectonophysics*, vol. 180, no. 2–4, pp. 237–254, 1990.
- [6] G. Igarashi, S. Saeki, N. Takahata et al., "Ground-water radon anomaly before the Kobe earthquake in Japan," *Science*, vol. 269, no. 5220, pp. 60–61, 1995.
- [7] L. Claesson, A. Skelton, C. Graham et al., "Hydro-geochemical changes before and after a major earthquake," *Geology*, vol. 32, no. 8, pp. 641–644, 2004.
- [8] J. Y. Liu, Y. I. Chen, C. H. Chen et al., "Seismoionospheric GPS total electron content anomalies observed before the 12 May 2008Mw7.9 Wenchuan earthquake," *Journal of Geophysical Research: Space Physics*, vol. 114, no. A4, 2009.
- [9] C. Y. Wang and M. Manga, "Hydrologic responses to earthquakes and a general metric," *Geofluids*, vol. 10, no. 1–2, pp. 206–216, 2010.
- [10] D. V. Reddy and P. Nagabhushanam, "Chemical and isotopic seismic precursory signatures in deep groundwater: cause and effect," *Applied Geochemistry*, vol. 27, no. 12, pp. 2348–2355, 2012.
- [11] A. Skelton, M. Andrén, H. Kristmannsdóttir et al., "Changes in groundwater chemistry before two consecutive earthquakes in Iceland," *Nature Geoscience*, vol. 7, no. 10, pp. 752–756, 2014.
- [12] Z. Shi, G. Wang, C. Y. Wang, M. Manga, and C. Liu, "Comparison of hydrological responses to the Wenchuan and Lushan earthquakes," *Earth and Planetary Science Letters*, vol. 391, pp. 193–200, 2014.
- [13] M. Lupi, B. S. Ricci, J. Kenkel et al., "Subsurface fluid distribution and possible seismic precursory signal at the Salse di Nirano mud volcanic field, Italy," *Geophysical Journal International*, vol. 204, no. 2, pp. 907–917, 2015.
- [14] A. Barkat, A. Ali, U. Hayat et al., "Time series analysis of soil radon in northern Pakistan: implications for earthquake forecasting," *Applied Geochemistry*, vol. 97, pp. 197–208, 2018.
- [15] S. Onda, Y. Sano, N. Takahata et al., "Groundwater oxygen isotope anomaly before the M6.6 Tottori earthquake in Southwest Japan," *Scientific Reports*, vol. 8, no. 1, p. 4800, 2018.
- [16] S. R. Paudel, S. P. Banjara, A. Wagle, and F. T. Freund, "Earthquake chemical precursors in groundwater: a review," *Journal of Seismology*, vol. 22, no. 5, pp. 1293–1314, 2018.
- [17] A. Barkat, A. Ali, N. Siddique, A. Alam, M. Wasim, and T. Iqbal, "Radon as an earthquake precursor in and around northern Pakistan: a case study," *Geochemical Journal*, vol. 51, no. 4, pp. 337–346, 2017.
- [18] V. Walia, T. F. Yang, S. J. Lin et al., "Temporal variation of soil gas compositions for earthquake surveillance in Taiwan," *Radiation Measurements*, vol. 50, pp. 154–159, 2013.
- [19] S. E. Ingebritsen and M. Manga, "Hydrogeochemical precursors," *Nature Geoscience*, vol. 7, no. 10, pp. 697–698, 2014.
- [20] H. Woith, "Radon earthquake precursor: a short review," *The European Physical Journal Special Topics*, vol. 224, no. 4, pp. 611–627, 2015.
- [21] A. Barkat, A. Ali, K. Rehman et al., "Multi-precursory analysis of phalla earthquake (July 2015; Mw 5.1) near Islamabad, Pakistan," *Pure and Applied Geophysics*, vol. 175, no. 12, pp. 4289–4304, 2018.
- [22] C. C. Fu, T. F. Yang, M. C. Tsai et al., "Exploring the relationship between soil degassing and seismic activity by continuous radon monitoring in the Longitudinal Valley of eastern Taiwan," *Chemical Geology*, vol. 469, pp. 163–175, 2017.
- [23] N. Ahmad, A. Barkat, A. Ali et al., "Investigation of spatio-temporal satellite thermal IR anomalies associated with the

- Awaran earthquake (Sep 24, 2013; M 7.7), Pakistan,” *Pure and Applied Geophysics*, vol. 176, no. 8, pp. 3533–3544, 2019.
- [24] Z. Shi, G. Wang, M. Manga, and C. Y. Wang, “Mechanism of co-seismic water level change following four great earthquakes - insights from co-seismic responses throughout the Chinese mainland,” *Earth and Planetary Science Letters*, vol. 430, pp. 66–74, 2015.
- [25] H. Zafrir, Y. Ben Horin, U. Malik, C. Chemo, and Z. Zalevsky, “Novel determination of radon-222 velocity in deep subsurface rocks and the feasibility to using radon as an earthquake precursor,” *Journal of Geophysical Research: Solid Earth*, vol. 121, no. 9, pp. 6346–6364, 2016.
- [26] A. Sciarra, A. Mazzini, S. Inguaggiato, F. Vita, M. Lupi, and S. Hadi, “Radon and carbon gas anomalies along the Watukosek fault system and Lusi mud eruption, Indonesia,” *Marine and Petroleum Geology*, vol. 90, pp. 77–90, 2018.
- [27] A. Skelton, L. Liljedahl-Claesson, N. Wästebý et al., “Hydro-chemical Changes Before and After Earthquakes Based on Long-Term Measurements of Multiple Parameters at Two Sites in Northern Iceland—A Review,” *Journal of Geophysical Research: Solid Earth*, vol. 124, no. 3, pp. 2702–2720, 2019.
- [28] G. Martinelli, *Fluidodynamical and chemical features of radon 222 related to total gases: implications for earthquake predictions*, IAEA, Vienna, Austria, 1993, (No. IAEA-TECDOC-726).
- [29] T. Lay, Q. Williams, and E. J. Garnero, “The core-mantle boundary layer and deep earth dynamics,” *Nature*, vol. 392, no. 6675, pp. 461–468, 1998.
- [30] K. Koike, T. Yoshinaga, K. Suetsugu, K. Kashiwaya, and H. Asaue, “Controls on radon emission from granite as evidenced by compression testing to failure,” *Geophysical Journal International*, vol. 203, no. 1, pp. 428–436, 2015.
- [31] H. Wakita, Y. Nakamura, K. Notsu, M. Noguchi, and T. Asada, “Radon anomaly: a possible precursor of the 1978 Izu-Oshima-kinkai earthquake,” *Science*, vol. 207, no. 4433, pp. 882–883, 1980.
- [32] T. L. Teng, L. F. Sun, and J. K. McRaney, “Correlation of groundwater radon anomalies with earthquakes in the Greater Palmdale Bulge area,” *Geophysical Research Letters*, vol. 8, no. 5, pp. 441–444, 1981.
- [33] P. F. Biagi, A. Ermini, S. P. Kingsley, Y. M. Khatkevich, and E. I. Gordeev, “Difficulties with interpreting changes in groundwater gas content as earthquake precursors in Kamchatka, Russia,” *Journal of Seismology*, vol. 5, no. 4, pp. 487–497, 2001.
- [34] V. I. Ulomov and B. Z. Mavashev, “Forerunners of the Tashkent earthquakes,” *Izvestia Akadamiyi Nauk Uzbekistan SSR*, pp. 188–200, 1971.
- [35] A. Riggio and M. Santulin, “Earthquake forecasting: a review of radon as seismic precursor,” *Bollettino di Geofisica Teorica ed Applicata*, vol. 56, no. 2, 2015.
- [36] C. B. Raleigh, G. Bennett, H. Craig et al., “Prediction of the Haicheng earthquake,” *EOS Transactions of the American Geophysical Union*, vol. 58, pp. 236–272, 1977.
- [37] H. ui, H. Moriuchi, Y. Takemura, H. Tsuchida, I. Fujii, and M. Nakamura, “Anomalously high radon discharge from the atotsugawa fault prior to the western nagano prefecture earthquake (m 6.8) of september 14, 1984,” *Tectonophysics*, vol. 152, no. 1-2, pp. 147–152, 1988.
- [38] K. Okumura, “Kobe earthquake of January 17, 1995 and studies on active faulting in Japan,” in *Extended Abstracts, 11th Course: Active Faulting Studies for Seismic Hazard Assessment*, International School Solid Earth Geophysics, Erice, Italy, 1995.
- [39] Y. Yin, F. Wang, and P. Sun, “Landslide hazards triggered by the 2008 Wenchuan earthquake, Sichuan, China,” *Landslides*, vol. 6, no. 2, pp. 139–152, 2009.
- [40] C. Liu, P. Dong, B. Zhu, and Y. Shi, “Stress shadow on the southwest portion of the Longmen Shan Fault impacted the 2008 Wenchuan earthquake rupture,” *Journal of Geophysical Research: Solid Earth*, vol. 123, no. 11, pp. 9963–9981, 2018.
- [41] Y. Xu, K. D. Koper, O. Sufri, L. Zhu, and A. R. Hutko, “Rupture imaging of the Mw7.9 12 May 2008 Wenchuan earthquake from back projection of teleseismic Pwaves,” *Geochemistry, Geophysics, Geosystems*, vol. 10, no. 4, 2009.
- [42] R. Q. Huang and W. L. Li, “Analysis of the geo-hazards triggered by the 12 May 2008 Wenchuan earthquake, China,” *Bulletin of Engineering Geology and the Environment*, vol. 68, no. 3, pp. 363–371, 2009.
- [43] P. Cui, X. Q. Chen, Y. Y. Zhu et al., “The Wenchuan earthquake (May 12, 2008), Sichuan province, China, and resulting geohazards,” *Natural Hazards*, vol. 56, no. 1, pp. 19–36, 2011.
- [44] M. Liu, Y. Yang, Z. Shen, S. Wang, M. Wang, and Y. Wan, “Active tectonics and intracontinental earthquakes in China: the kinematics and geodynamics,” *Continental Intraplate Earthquakes: Science, Hazard, and Policy Issues*, vol. 425, 2007.
- [45] Z. Q. Ming, G. Hu, X. Jiang, S. C. Liu, and Y. L. Yang, *Catalog of Chinese Historic Strong Earthquakes from 23 A.D. to 1911*, Seismological Publishing House, Beijing, 1995.
- [46] Y. Chen, K. L. Tsoi, F. B. Chen, Z. H. Gao, Q. J. Zou, and Z. L. Chen, *The Great Tangshan Earthquake of 1976: An Anatomy of Disaster*, Pergamon Press, Oxford, 1988.
- [47] P. Tapponnier and P. Molnar, “Active faulting and tectonics in China,” *Journal of Geophysical Research*, vol. 82, no. 20, pp. 2905–2930, 1977.
- [48] P. Z. Zhang, Q. Deng, G. M. Zhang et al., “Strong earthquakes and crustal block motion in continental China,” *Science in China*, vol. 33, pp. 12–20, 2003.
- [49] Y. Ran, L. Chen, J. Chen et al., “Paleoseismic evidence and repeat time of large earthquakes at three sites along the Longmenshan fault zone,” *Tectonophysics*, vol. 491, no. 1-4, pp. 141–153, 2010.
- [50] B. Zhao, Y. Shi, and Y. Gao, “Relocation of aftershocks of the Wenchuan MS8.0 earthquake and its implication to seismotectonics,” *Earthquake Science*, vol. 24, no. 1, pp. 107–113, 2011.
- [51] H. W. Ren, Y. W. Liu, and D. Y. Yang, “A preliminary study of post-seismic effects of radon following the Ms 8.0 Wenchuan earthquake,” *Radiation Measurements*, vol. 47, no. 1, pp. 82–88, 2012.
- [52] S. M. Barbosa, H. Zafrir, U. Malik, and O. Piatibratova, “Multiyear to daily radon variability from continuous monitoring at the Amram tunnel, southern Israel,” *Geophysical Journal International*, vol. 182, no. 2, pp. 829–842, 2010.
- [53] J. Planinić, B. Vuković, and V. Radolić, “Radon time variations and deterministic chaos,” *Journal of Environmental Radioactivity*, vol. 75, no. 1, pp. 35–45, 2004.
- [54] R. Yan, H. Woith, R. Wang, and G. Wang, “Decadal radon cycles in a hot spring,” *Scientific Reports*, vol. 7, no. 1, p. 12120, 2017.
- [55] R. V. Donner, S. M. Potirakis, S. M. Barbosa, J. A. O. Matos, A. J. S. C. Pereira, and L. J. P. F. Neves, “Intrinsic vs. spurious long-range memory in high-frequency records of

- environmental radioactivity,” *The European Physical Journal Special Topics*, vol. 224, no. 4, pp. 741–762, 2015.
- [56] C. Barman, H. Chaudhuri, A. Deb, D. Ghose, and B. Sinha, “The essence of multifractal detrended fluctuation technique to explore the dynamics of soil radon precursor for earthquakes,” *Natural Hazards*, vol. 78, no. 2, pp. 855–877, 2015.
- [57] I. P. Dobrovolsky, S. I. Zubkov, and V. I. Miachkin, “Estimation of the size of earthquake preparation zones,” *Pure and Applied Geophysics*, vol. 117, no. 5, pp. 1025–1044, 1979.
- [58] M. Hamdache, J. Henares, J. A. Peláez, and Y. Damerdj, “Fractal analysis of earthquake sequences in the Ibero-Maghrebian region,” *Pure and Applied Geophysics*, vol. 176, no. 4, pp. 1397–1416, 2019.
- [59] B. R. Arora, A. Kumar, V. Walia et al., “Assesment of the response of the meteorological/hydrological parameters on the soil gas radon emission at Hsinchu, northern Taiwan: a prerequisite to identify earthquake precursors,” *Journal of Asian Earth Sciences*, vol. 149, pp. 49–63, 2017.
- [60] M. Awais, A. Barkat, A. Ali, K. Rehman, W. Ali Zafar, and T. Iqbal, “Satellite thermal IR and atmospheric radon anomalies associated with the Haripur earthquake (Oct 2010; $M_w=5.2$), Pakistan,” *Advances in Space Research*, vol. 60, no. 11, pp. 2333–2344, 2017.
- [61] Y. H. Oh and G. Kim, “A radon-thoron isotope pair as a reliable earthquake precursor,” *Scientific Reports*, vol. 5, no. 1, 2015.
- [62] Q. Ye, R. P. Singh, A. He, S. Ji, and C. Liu, “Characteristic behavior of water radon associated with Wenchuan and Lushan earthquakes along Longmenshan fault,” *Radiation Measurements*, vol. 76, pp. 44–53, 2015.